International Journal of Biological Macromolecules xxx (xxxx) xxx

Contents lists available at ScienceDirect

International Journal of Biological Macromolecules

journal homepage: www.elsevier.com/locate/ijbiomac

Effects of environmental stimuli on the physicochemical and rheological properties of chitosan-macroalgal polyphenol stabilized Pickering emulsion

Weihao Meng [a,b,1], Hongnan Sun [a,*,1], Taihua Mu [a,*], Marco Garcia-Vaquero [b,*]

[a] Laboratory of Food Chemistry and Nutrition Science, Institute of Food Science and Technology, Chinese Academy of Agricultural Sciences, Key Laboratory of Agro-Products Processing, Ministry of Agriculture and Rural Affairs, No. 2 Yuan Ming Yuan West Road, Haidian District, P.O. Box 5109, Beijing 100193, PR China
[b] School of Agriculture and Food Science, University College Dublin, Belfield, Dublin 4, Ireland

ARTICLE INFO

Keywords:
Pickering emulsion
Chitosan
Macroalgal polyphenols
Environmental stimuli
Emulsion stability

ABSTRACT

In this study, Pickering emulsions stabilized by chitosan (CS), chitosan-*Laminaria japonica* polyphenols (CP) and chitosan-*Ascophyllum nodosum* polyphenols (CB) were fabricated. This study also evaluated the stability of CS, CP, and CB under different environmental factors including pH (2–9), NaCl concentrations (0–500 mM), heat treatments (50–100 °C) and storage period (0–8 weeks). The characterization on interfacial layer of emulsion droplets demonstrated that macroalgal polyphenols could combined with the amorphous regions of chitosan particles through hydrogen bond and electrostatic interactions, providing stronger dual wettability with enhanced ability of interfacial layer in stabilizing Pickering emulsions. All three emulsions showed best droplet distribution, highest emulsion stability and specific surface area at pH 6 and 0 mM NaCl concentration as fresh emulsion. Moreover, CS, CP, and CB exhibited the rheological behaviour of pseudoplastic fluids at different pH and NaCl concentration. It should be noted that CP and CB exhibited higher emulsion stability than CS under a variety of environmental stresses. Overall, this research proved that chitosan-macroalgal polyphenol co-stabilized Pickering emulsion had enhanced stability against various environmental stimuli, which could be utilized as potential delivery and protection system for hydrophobic bioactive compounds.

1. Introduction

Food-grade Pickering emulsions are currently gaining momentum in the functional food sector as they can act as biocompatible and biodegradable stabilizers of bioactive compounds, protecting them to reach their target organs [1]. High energy inputs are regularly required to dissociate stabilizer particles from the interface of Pickering emulsions and thus, these systems are generally considered to be extremely stable before the preservation of bioactive compounds at their oil phase during extended periods of time [2]. Chitosan is a cationic polysaccharide that is Generally Recognized as Safe (GRAS) by the US Food and Drug Administration (U.S. FDA) with multiple applications, including its use as food additive, drug delivery and dietary supplement due to its relatively inexpensive price, high market availability, and biocompatibility [3–5]. Although chitosan can self-aggregate and act as a Pickering emulsion stabilizer, its strong hydrophilicity limits its stability in response to environmental stimuli [6,7]. Recent studies have shown that Pickering emulsions stabilized by chitosan and other polymers have higher stability than only by chitosan nanoparticles [8]. Layer-by-layer electrostatic deposition is an efficient and promising technique for developing co-stabilized emulsion systems by using two oppositely charged stabilizers deposited at the oil-water interface to improve emulsion stability [9].

Moreover, recent studies have shown that chitosan-based Pickering emulsions have many attractive and innovative applications in the delivery systems for several hydrophobic bioactive ingredients such as curcumin [10], lycopene [11], resveratrol [12], rutin [13], eicosapentaenoic acid (EPA) [14], and essential oil [15]. It is worth noting that the industrial application of Pickering emulsion as a food ingredient is very complicated, while many external environmental factors (such as pH, ionic strength, temperature, and storage time) could affect its properties [16]. Therefore, before the Pickering emulsion is applied to complex food systems, its stability against different external environments should be explored to further prove its potential application prospects.

Brown macroalgae (Phaeophyceae), such as *Laminaria japonica* and

* Corresponding authors.
E-mail addresses: honey0329@163.com (H. Sun), mutaihua@126.com (T. Mu), marco.garciavaquero@ucd.ie (M. Garcia-Vaquero).
[1] These authors contributed equally: Weihao Meng and Hongnan Sun.

https://doi.org/10.1016/j.ijbiomac.2022.11.314
Received 29 September 2022; Received in revised form 20 November 2022; Accepted 29 November 2022
Available online 5 December 2022

Ascophyllum nodosum are exploited worldwide, being mainly produced by China and Chile [17]. Moreover, brown macroalgae have been recently explored as a source of multiple compounds, such as polyphenols, that can display a wide array of health benefits including antioxidant [17], antimicrobial [18], and anti-inflammatory [19], antihypertensive [20], antidiabetic [21], and anticancer activities [22]. Despite the huge potential of macroalgal polyphenols and their potential health benefits, the use of these compounds as pharmaceuticals, cosmeceuticals, nutraceuticals and functional foods is still limited [17,23]. Numerous studies have shown that polyphenols from multiple sources can act as effective stabilizers for oil in water (O/W) emulsions [2,6] and thus, exploring the use of these compounds as Pickering emulsion stabilizers could contribute to broaden the utilization of these molecules as food additives or ingredients. In our previous study [24], the preparation process of Pickering emulsions co-stabilized by chitosan and macroalgal polyphenols from *Ascophyllum nodosum* by layer-by-layer electrostatic deposition was optimised. However, there is still limited understanding of how this novel chitosan-macroalgal polyphenol co-stabilized emulsions respond to environmental stimuli that will be necessary to determine the stability and the future processing conditions of these emulsions needed when formulating novel foods and other uses by the pharmaceutical and cosmeceutical industries.

This study aims to characterize the binding properties between chitosan and polyphenols from different macroalgal species by Fourier transform infrared spectroscopy (FTIR), X-ray diffraction (XRD), contact angle, and transmission electron microscopy (TEM) when developing Pickering emulsions. At the same time, the effect of environmental stimuli (pH, ionic strength, heat treatment, and storage period) on the morphology, stability, droplets specific surface area and rheology properties of emulsions were also determined. This study demonstrated the potential advantage of chitosan-macroalgal polyphenols stabilized Pickering emulsion against various environment effects than emulsion stabilized only by chitosan particles as delivery systems of hydrophobic bioactive compounds. Moreover, this research also explored further applications of naturally extracted polyphenols in innovative emulsion with future applications in the pharmaceutical, cosmeceutical and food industries, beyond those commonly explored of inclusion in food formulations directly.

2. Materials and methods

2.1. Biological materials and chemical reagents

Macroalgal *A. nodosum* was purchased from the Qingdao Mingyue Company (Qingdao, Shandong, China). Polyphenols from *A. nodosum* were prepared by ultrasonic assisted enzymatic extraction and liquid-liquid participation, the extract which was not soluble in water and *n*-hexane was collected with purity of 73.85 % (Meng et al., not published yet). Polyphenols from *L. japonica* (84.13 % purity) were purchased from Xi'an Baichuan Technology Co. Ltd. (Xi'an, Shaanxi, China).

Low molecular weight (MW) chitosan (MW ranging from 50 to 190 kDa, deacetylation degree of 75–85 %) and Nile Red were purchased from Sigma-Aldrich, Inc. (St. Louis, MO, USA). Other reagents were of analytical grade and purchased from Beijing Chemical Reagents Co. (Beijing, China). Deionized water with a resistivity of not $<$18.2 MΩ was used in all experiments. Corn oil for the preparation of emulsions was purchased from Arawana (Beijing, China).

2.2. Preparation of chitosan and macroalgal polyphenol solution

Chitosan powder was dissolved in an aqueous HCl solution (pH 3) under magnetic stirring at 300 rpm for 4 h (HJ-6, Changzhou Zhongbei Instrument Co. Ltd., Changzhou, Jiangsu, China), and then adjusted pH to 6 by adding 1 M NaOH and incubated overnight at room temperature to generate chitosan dispersions (1 %, w/v, zeta potential: 25.7 mV). Macroalgal polyphenols dispersions (1 %, phenolic content/v, zeta potential: −37.4 mV (*L. japonica*) and −34.6 mV (*A. nodosum*)) were prepared using an ultrasonic bath (SK8210HP, Kudos, Shanghai, China) at 53 kHz, 500 W, 25 °C for 15 min to disperse polyphenols in an aqueous HCl solution at pH 6.

2.3. Preparation of emulsions

Chitosan stabilized Pickering emulsions (CS), chitosan-*L. japonica* polyphenols stabilized Pickering emulsions (CP), and chitosan-*A. nodosum* polyphenols stabilized Pickering emulsions (CB) were generated based on the layer-by-layer electrostatic deposition method following the protocol as developed by our previous research [24]. Briefly, the chitosan and polyphenol dispersions are diluted to the desired concentration. Then, 165 mL of chitosan dispersion was mixed with 15 mL of corn oil, and then mixed at 10,000 rpm for 1 min using high-speed homogenizer (I25, IKN Co., Shanghai, China) and then homogenized 3 cycles with a high-pressure homogenizer (D-3L, PhD Technology LLC, USA) at a pressure of 60 MPa to prepare the primary emulsion. 120 mL of water or macroalgal polyphenol dispersion were slowly added to the primary Pickering emulsion, respectively. The mixtures were homogenized at 10,000 rpm for 1 min, and then 3 cycles at 60 MPa using a high-pressure homogenizer to prepare CS, CP and CB, respectively. The final chitosan concentration was 0.5 % (w/v), and the ratio of chitosan to macroalgal polyphenols was 9.5:1 (chitosan content: phenolic content) in each type of emulsion. The pH of CS, CP and CB were 5.86, 5.96, and 5.94, respectively. Zeta potential of these emulsions were 20.6 mV (CS), 16.4 mV (CP), and 17.5 mV (CB), respectively.

2.4. Characterization of emulsion stabilizers

2.4.1. Separation of interfacial layer stabilizers

The methods of interfacial layer stabilizers separation was referred to [25] with slightly modification. Briefly, emulsions were centrifuged at 10,000 *g* for 20 min at 4 °C and then mixed with *n*-hexane at 65 °C for 30 min for oil removal. The *n*-hexane fraction was separated at 10,000 *g* centrifugation for 20 min at 4 °C. The interfacial layer stabilizers were collected and freeze-dried for further research.

2.4.2. Fourier transform infrared spectroscopy (FTIR) analysis

FTIR analyses were performed as described by [26] with slightly modifications. Briefly, interfacial layer of CS, CP, and CB were triturated with potassium bromide (KBr) to yield pellets, respectively. The FTIR absorbance spectrum at IR ranges of 600 and 4000 cm^{-1} with a resolution of 2 cm^{-1} were recorded by Tensor 27 FTIR spectrometer (Bruker, Karlsruhe, Germany).

2.4.3. X-ray diffraction (XRD)

XRD were determined by an X-ray diffractometer (Brucker D8 Advance, Germany) as described by [10] with slightly modification. The instrument was equipped with a copper anode that produced Cu Kα radiation, and was operated at 40 kV of an accelerating voltage (wavelength: 1.5418 Å). 2θ was set from 2° to 60° with scanning rate as 2°/min.

2.4.4. Contact angle

Contact angles of interfacial layer of CS, CP and CB were obtained with a DSA 30 Contact Angle System (with goniometer equipped with a system of drop shape analysis, Krüss, Germany).

2.4.5. Transmission electron microscopy (TEM)

The morphology of stabilizers of CS, CP, and CB were investigated by TEM (H-7500, Hitachi, Tokyo, Japan) with 80 kV voltages. The emulsion stabilizers were diluted to 10 μg/mL with deionized water. A droplet of diluted solution dispersion was put onto a carbon support film on a copper grid and allowed to dry in air. Particle dimension was determined by ImageJ software.

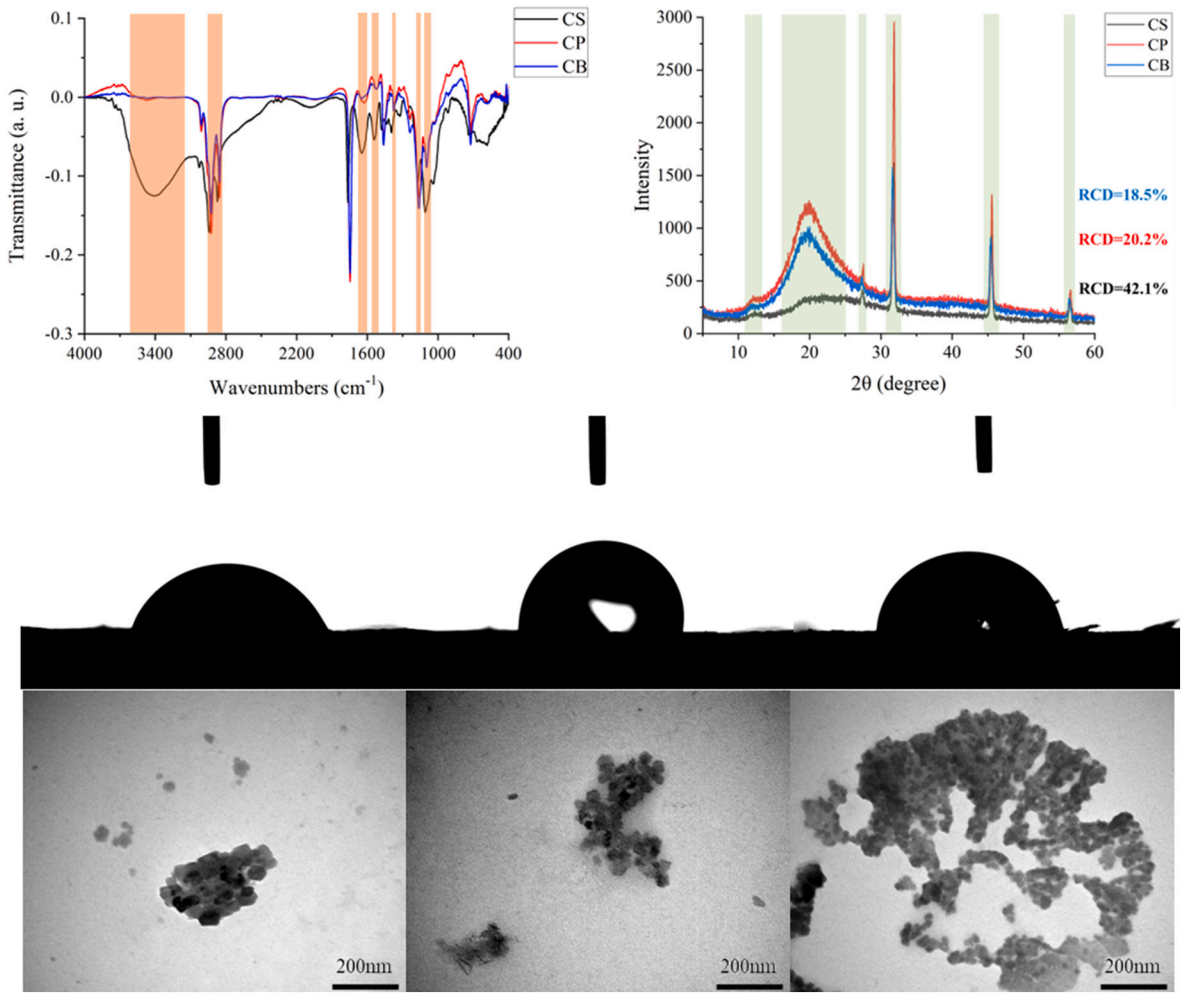

Fig. 1. (A) FTIR spectra, (B) XRD, contact angle of (C) CS, (D) CP, and (E) CB and TEM of (F) CS, (G) CP, and (H) CB.

2.5. Application of environmental stresses and characterization of emulsions

Once the emulsions were generated, they were subjected to several environmental stresses aiming to determine their stability under different processing conditions. The effect of the pH on Pickering emulsions was studied by adjusting the pH of the emulsions to 2, 4, 6, 7, and 9 using 0.1 M HCl or NaOH solutions. The ionic strength of Pickering emulsions was tested by the addition of 0, 100, 300 and 500 mM of NaCl. The heat stability was tested by heating the emulsions to 50, 60, 70, 80, 90, and 100 °C using a water bath (DSHZ-300A, Taicang Experimental Equipment Factory, Taicang, Jiangsu, China) for 30 min followed by cooling down to room temperature. The storage stability of Pickering emulsions was also tested by storing all the emulsions at 25 ± 1 °C for 8 weeks.

Optical microscopy, macroscopic observation, emulsion physical stability, droplet size distribution. Rheology properties and multiple light scattering stability were used to characterize these environmental stresses on emulsions.

2.5.1. Optical microscope observation of emulsion

Optical microscopic observations were performed as described by [27] with some modifications. 0.5 mL of emulsions were transferred into 4.5 mL of deionized water, and vortexed for 5 s. 20 μL mixtures were carefully placed between the microscope slide and the cover glass. The microscopic morphology of the droplets was evaluated using an optical microscope (CX41, Olympus Corporation, Tokyo, Japan) equipped with a 40× magnification objective lens and a 10× magnification eyepiece. The images were recorded by CCD camera (EOS 450D, Canon, Japan).

2.5.2. Macroscopic observations

Macroscopic observation were performed based on [28] with slightly changes. 7 mL of fresh emulsion was pipetted into a 10 mL clear glass bottle accurately and screw the cap tightly to seal it. Emulsions were stored 12 h at room temperature or during storage period. Macroscopic observations of each emulsion were taken by CCD camera aiming to determine the water and/or oil phase delamination.

2.5.3. Emulsion physical stability

Emulsion physical stability was determined referred to [29] with slightly changes. Briefly, 10 mL of fresh emulsion was centrifuged at 3000 *g* for 15 min at 4 °C. Emulsion physical stability was measured based on the following equations:

$$\text{Emulsion physical stability } (\%) = \frac{\text{Final emulsion volume}}{\text{Initial emulsion volume}} \times 100 \quad (1)$$

2.5.4. Measurement of specific surface area

The specific surface area of emulsion droplets was measured by laser particle size analyser (Bettersizer 2000, Dandong Bettersize Instrument Co., Ltd., Dandong, Liaoning, China) as indicated by [30] with slightly modifications. 0.5 mL of emulsions was diluted in 400 mL solutions with the same pH or NaCl deionized water to avoid the influence of light scattering caused by dispersant before measurements. The relative refractive index of the emulsion was taken as 1.107, corresponding to

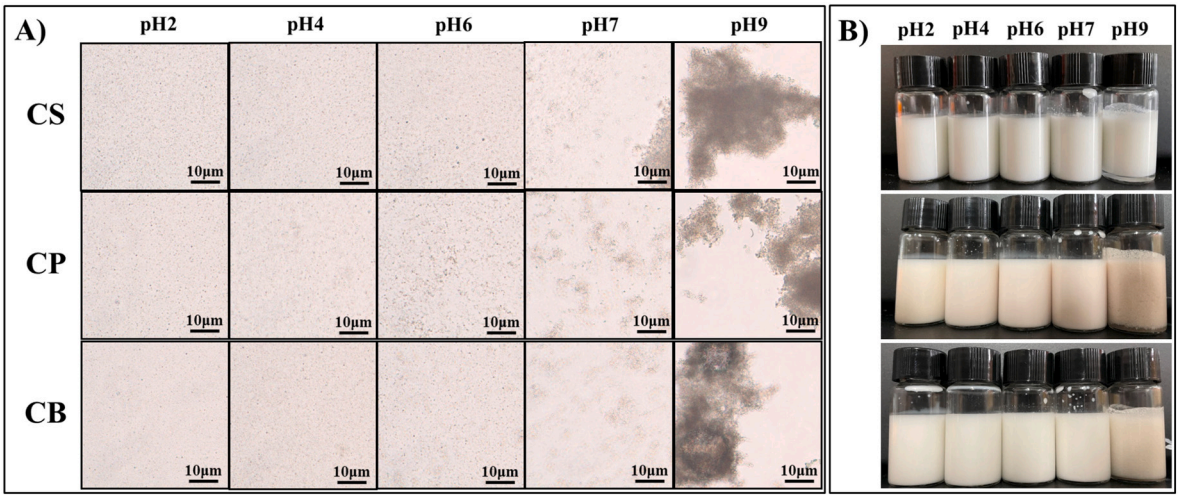

Fig. 2. Images of the evaluation of Pickering emulsions stabilized with chitosan (CS), chitosan-*Laminaria japonica* polyphenols (CP) and chitosan-*Ascophyllum nodosum* polyphenols (CB) at different pH values (2, 4, 6, 7 and 9). Images correspond to (A) optical microscopic evaluation and (B) macroscopic evaluation. The bars in the images represent 10 μm.

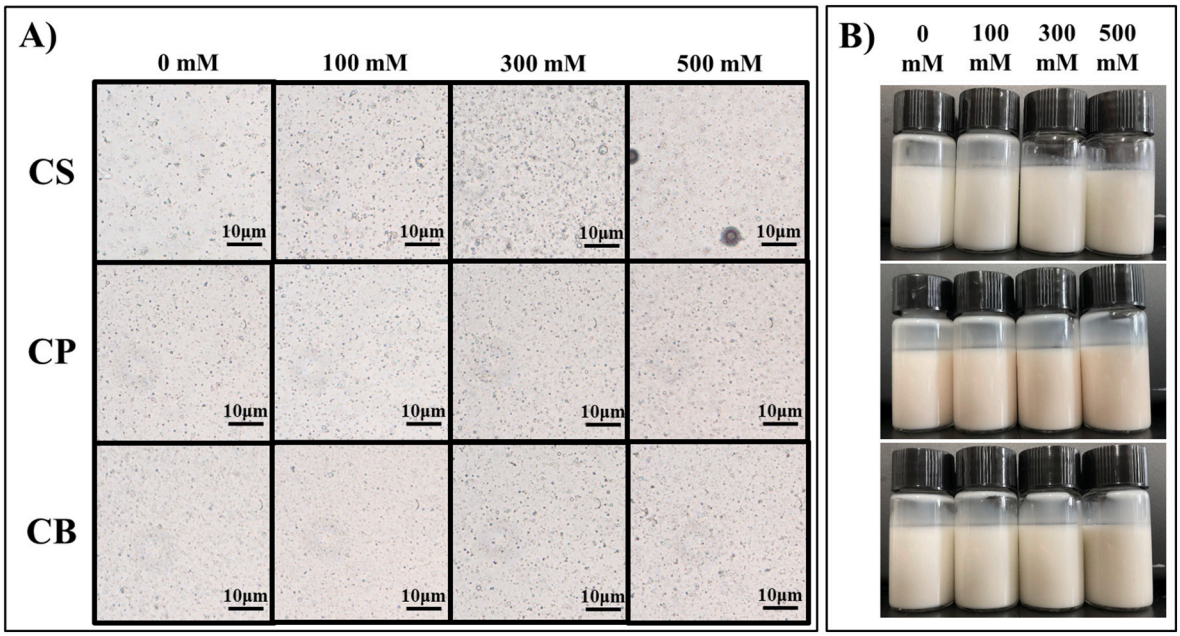

Fig. 3. Images of the evaluation of Pickering emulsions stabilized with chitosan (CS), chitosan-*Laminaria japonica* polyphenols (CP) and chitosan-*Ascophyllum nodosum* polyphenols (CB) at different NaCl concentrations (0, 100, 300, and 500 mM). Images correspond to (A) optical microscopic evaluation and (B) macroscopic evaluation. The bars in the images represent 10 μm.

the ratio of the refractive indices of corn oil and the deionized water (1.472 and 1.33, respectively).

2.5.5. Rheological properties

The rheological properties of the emulsions were determined as referred by [27] with slightly modifications. Briefly, the rheological properties of the emulsions at different pH and NaCl concentration were performed using an Anton Paar rheometer (Physica MCR 301, Austria) with a Peltier system temperature controller (HePTD 200) and a parallel plate geometry (PP50, 50 mm diameter, and a 0.500 mm gap). For each measurement, 1.20 mL of fresh emulsions were carefully deposited over the plate of the rheometer. When the emulsions contacted with the parallel plate geometry, the emulsions were equilibrated for 30 s and then were taken in a steady-rate flow mode with shear rate ranging from 0.01 to 100 s^{-1} during 15 min. The apparent viscosity of the emulsions was expressed as a viscosity value at a shear rate of 100 s^{-1}.

2.5.6. Multiple light scattering stability analysis

Multiple light scattering stability analysis was performed using a Turbiscan Lab instrument (Formulaction Co., L'Union, France) as indicated by [31] with slight modifications. Multiple light scattering stability analysis is an important approach to assess the combined effects of multiple environmental factors. Therefore, 20 mL of emulsions at different pH and NaCl concentration were placed in a flat-bottomed cylindrical glass tube. The backscattering (BS) and transmission (T) data were recorded for 6 h at 15 min intervals at the wavelength of 880 nm and 50 °C. Turbiscan stability index (TSI) was calculated according to the change of T and BS intensity by Turbiscan Tower software (Formulaction Co., L'Union, France) using Eq. (2).

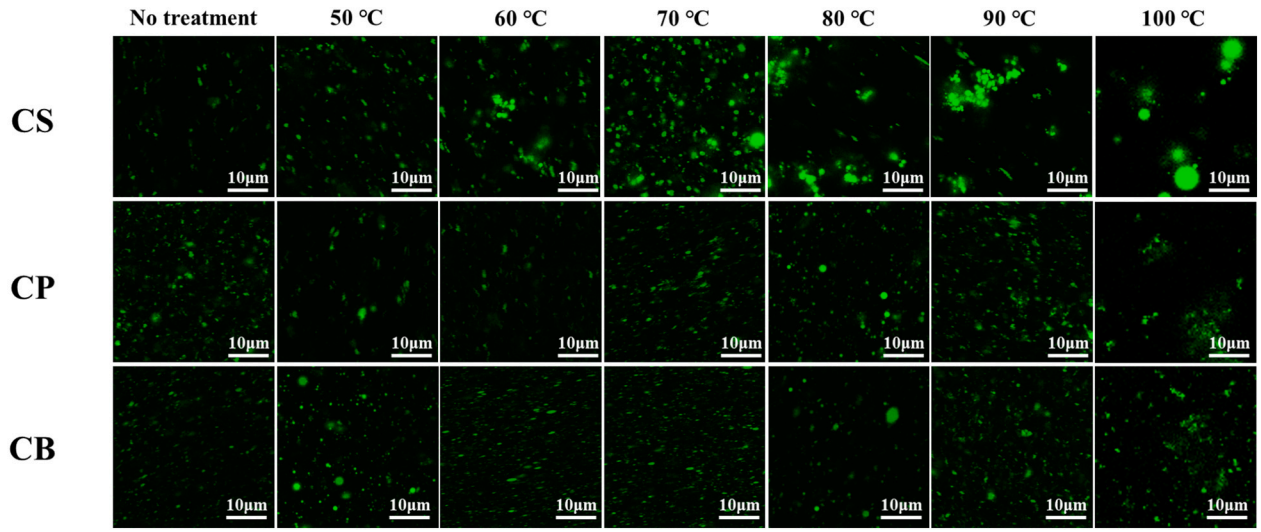

Fig. 4. CLSM of Pickering emulsions stabilized with chitosan (CS), chitosan-*Laminaria japonica* polyphenols (CP) and chitosan-*Ascophyllum nodosum* polyphenols (CB) at different heat treatments. The oil phase is shown in green in all the images and the scale bars are represented in red colour in the bottom left of the images representing 10 μm.

$$TSI = \sum_{i} \frac{\sum_{h} |scan_i(h) - scan_{i-1}(h)|}{H} \quad (2)$$

where $scan_i(h)$ is the average backscattering for each time (i) of measurement, $scan_{i-1}(h)$ is average backscattering for the time $(i - 1)$ of measurement, and H is the height of the sample.

TSI can be used to characterize the combined effects of multiple instability phenomena by the changes in light intensity [32]. In the emulsification process, flocculation and aggregation are the main factors affecting emulsification, and the higher TSI related to poorer stability [33].

2.5.7. Confocal laser scanning microscopy (CLSM)

Microstructure of the emulsions were visualized by confocal scanning laser microscope (TCS SP8, with 63 × objective lens, Leica Microsystems, Heidelberg, Germany) as described by [7] with slight modifications. 1 mL of emulsions were stained with 50 μL of a blended fluorescent colorant solution consisting of Nile Red (1 mg/mL) for 1 h. The dyed samples were diluted 10 times and 20 μL of diluted samples were carefully transferred onto the concave glass slide and covered with a glass cover slip (Citotest labware manufacturing Co., LTD, Haimen, Jiangsu, China). Nile red staining the oil phase were visualized at excitation wavelength of 514 nm. The optical resolution of the obtained digital images was 2048 pixels × 2048 pixels.

2.6. Statistical analyses

All measurements were performed in triplicate. Results were expressed as mean ± standard deviation (SD). One-way ANOVA and Duncan's multiple range tests were conducted to identify differences inside each treatment group using SPSS version 27.0 (IBM, Armonk, NY, USA). In all cases, the criterion for statistical significance was $P < 0.05$.

3. Results and discussion

3.1. Characterization of emulsion stabilizers

3.1.1. FTIR

FTIR spectra of the CS, CP and CB interfacial layer stabilizers were presented in Fig. 1A. The characteristic spectra of CS were as follows: 3412.0 cm^{-1} (O—H stretch overlapped with N—H stretch), 2943.3 and 2871.9 cm^{-1} (C—H stretch), 1645.2 cm^{-1} (amide I band, C═O stretch), 1541.1 cm^{-1} (amide II band, NH2 bending), 1394.5 cm^{-1} (amide III band, C—N stretch), 1172.7 cm^{-1} (C—O—C asymmetric stretching vibration) and 1109.0 cm^{-1} (C—O stretch), similar to the previously reported chitosan spectrum [34,35]. In CP and CB, the decrease in the intensity of the peak located at 3412.0 cm^{-1} of CS indicated the generation of hydrogen bonds between macroalgal polyphenols and chitosan [36]. Moreover, the peak position of the amide I band of chitosan particles was significantly shifted from 1645.2 cm^{-1} (CS) to 1625.9 cm^{-1} (CP and CB), while the amide II band was shifted from 1541.1 cm^{-1} (CS) to 1523.7 (CP) and 1521.8 cm^{-1} (CB). At the same time, the intensity of these two peaks also showed decrease trend after macroalgal addition. The reason for the change in peak position and intensity was the electrostatic interaction of NH_3^+ of chitosan with macroalgal polyphenols [37]. Overall, FTIR analyses suggested that chitosan and macroalgal polyphenols was combined by intermolecular hydrogen bonds and electrostatic interactions.

3.1.2. XRD

The XRD of stabilizers of CS, CP, and CB were shown in Fig. 1B. The interfacial layer of CS had two broad peaks with low intensity at $2\theta = 11.2°$ and 20.0°, which reflected the destruction of the natural chitosan stacking structure by strong intermolecular forces during the preparation of the emulsion [38,39]. Compared with CS, both CP and CB had broad peaks around 20°, which was due to the binding of macroalgae polyphenols to the amorphous region of chitosan, contributing to lower relative crystallinity degree (RCD) of CP (18.5 %) and CB (20.2 %) than that of CS (42.1 %). Similar results were also consistent with the change trend of chitosan combined with substances such as ascorbyl palmitate [40] and gum Arabic [41]. In CS, CP and CB, crystalline regions located at 27°, 32°, 46° and 57° all existed, indicating that the addition of macroalgal polyphenols did not change the structure of these crystal planes. Similar crystalline XRD diffraction peaks were also observed in chitosan from fishery waste [35] and chitosan-silver nanoparticles [42]. The results of XRD determined that macroalgal polyphenol bond to the amorphous region of the chitosan particles without affecting the crystalline region structure.

3.1.3. Contact angle

As Pickering emulsion stabilizer, chitosan particles had strong hydrophilicity, and was considered that certain modifications are needed to improve dual wettability [43]. The oil/water three-phase contact

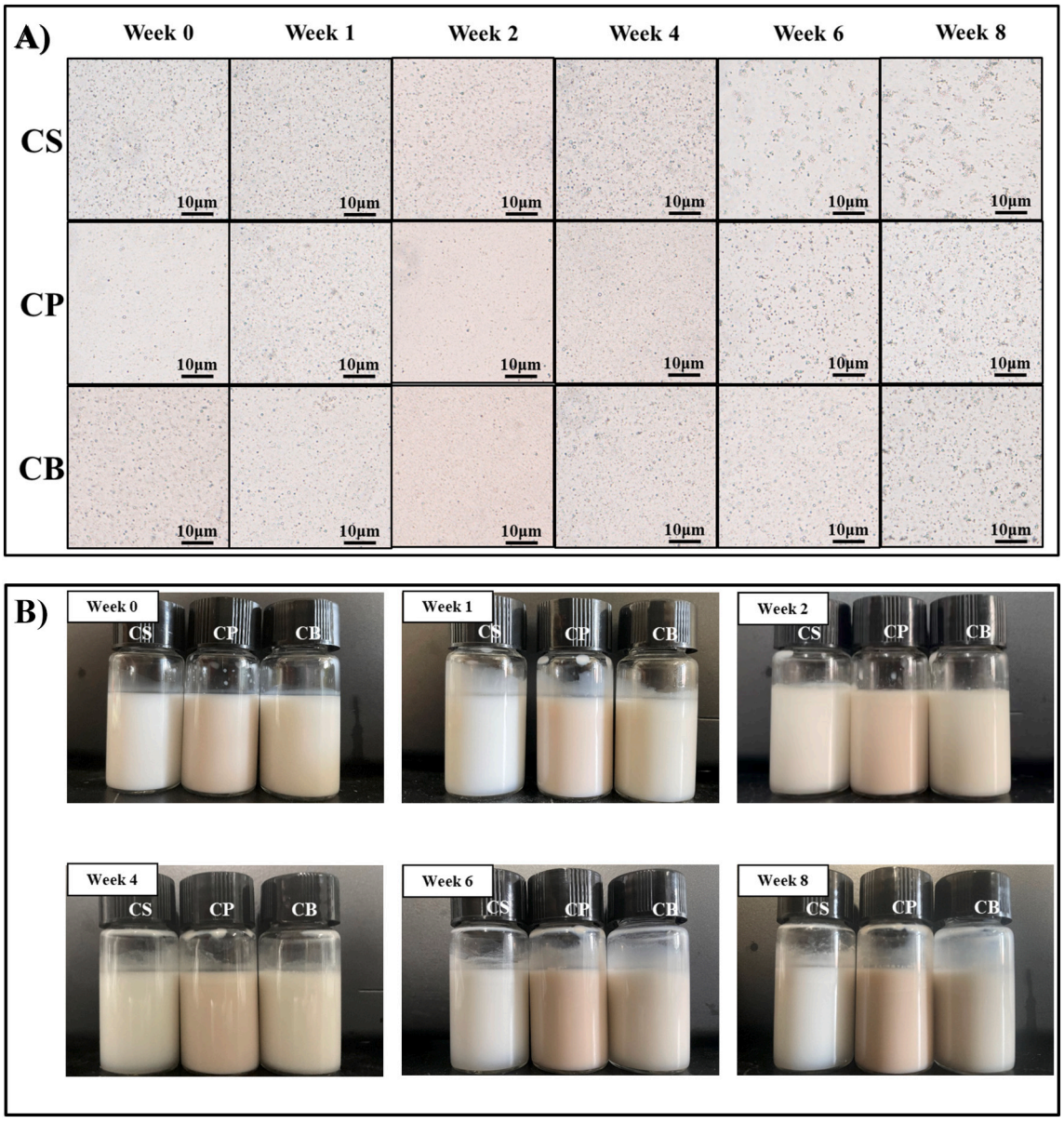

Fig. 5. Images of the evaluation of Pickering emulsions stabilized with chitosan (CS), chitosan-*Laminaria japonica* polyphenols (CP) and chitosan-*Ascophyllum nodosum* polyphenols (CB) at storage period ranging from 0 to 8 weeks. Images correspond to (A) optical microscopic evaluation and (B) macroscopic evaluation. The bars in the images represent 10 μm.

angles ($\theta_{o/w}$) of CS, CP, and CB was shown in Fig. 1C, D, E, respectively. Interfacial layer of CP (91.5°) and CB (87.8°) had higher $\theta_{o/w}$ than CS (69.0°), indicating their better ability to stabilize Pickering emulsion as $\theta_{o/w}$ approaching 90° [44]. Therefore, the conclusion of the contact angle proved that the addition of polyphenols leaded to the weakening of the hydrophilicity of chitosan particles as well as provided better hydrophilic-hydrophobic balance and dual wettability. Thus, CP and CB may also have stronger stability than CS when dealing with external environmental stimuli.

3.1.4. TEM

TEM images of CS, CP, and CB were shown in Fig. 1F, G, H, respectively, the interfacial layers of the three emulsions were all composed of particles. The mean diameters of the interfacial layer particles of the three Pickering emulsions were 21.81 nm (CS), 28.46 nm (CP), 23.62 nm (CB), respectively. These results were similar to the chitosan nanoparticles diameters of 25–50 nm previously reported by [40]. Moreover, particles of CP and CB showed better cross-linking than CS, which was because of the electrostatic adsorption of polyphenols with chitosan. It is worth noting that chitosan and polyphenol did not form new particles to stabilize Pickering emulsions during the preparation of emulsions. This phenomenon indicated that the electrostatic adsorption between chitosan and polyphenols in the emulsion is at the interface layer rather than bonded by hydrogen bonds to form a new solid particle. Overall, the results of TEM showed the polyphenol and chitosan particles interact with each other to stabilize the oil-water interface.

3.2. Effects of pH values on emulsion properties

3.2.1. Morphology

Emulsions may experience various pH conditions during manufacturing and digestion, which played a crucial role in the degree of ionization of the pendant functional groups carried by biopolymers [16]. The droplet optical microscope observation of emulsions with different pH was shown in Fig. 2A. At pH range was 2–6, all fresh

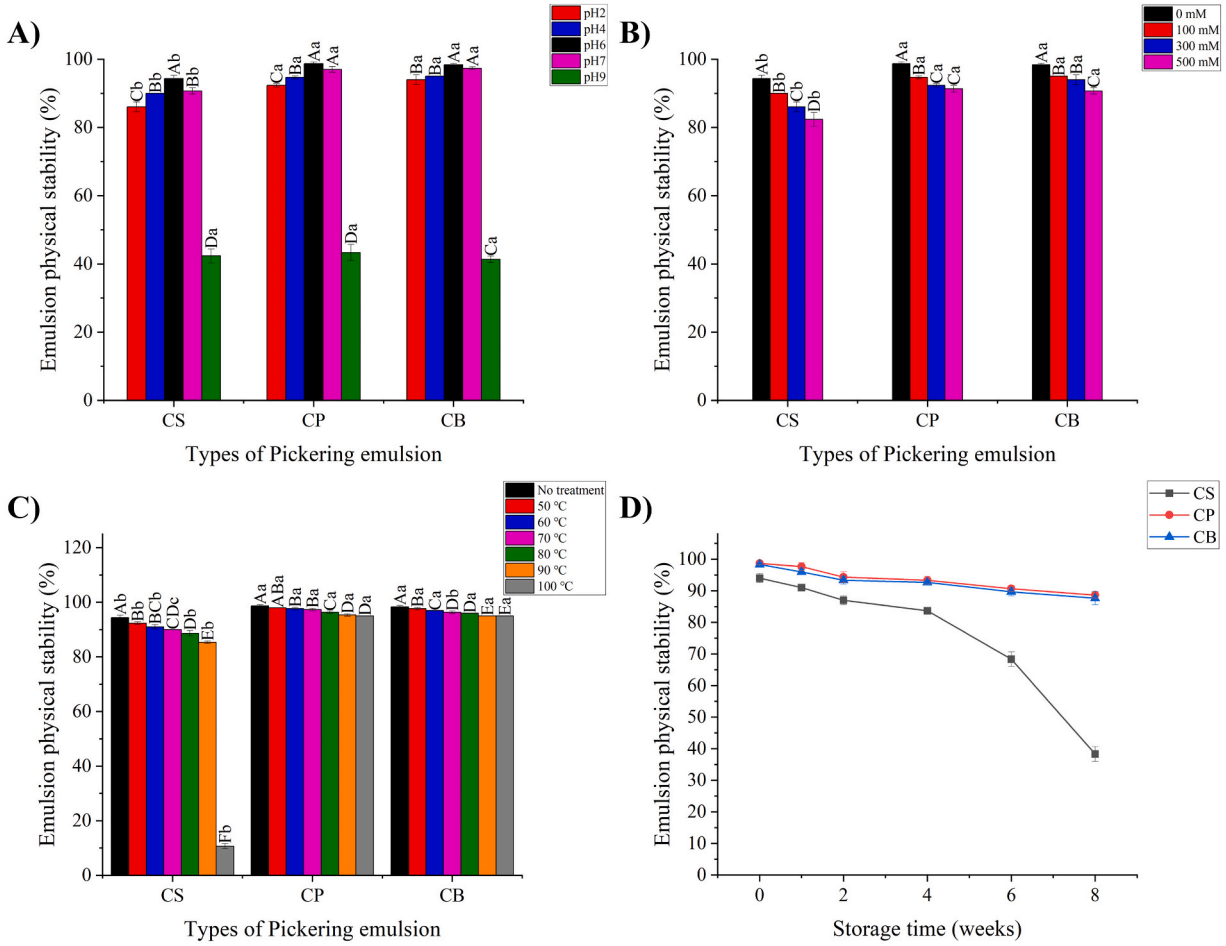

Fig. 6. Emulsion physical stability of Pickering emulsions stabilized with chitosan (CS), chitosan-*Laminaria japonica* polyphenols (CP) and chitosan-*Ascophyllum nodosum* polyphenols (CB) at different (A) pH values (2–9), (B) NaCl concentrations (0–500 mM), (C) heat processing conditions (control, 50–100 °C), (D) storage period (0–8 weeks). Different uppercase or lowercase letters statistically significant differences ($P < 0.05$) in emulsion physical stability within the same emulsion type under different environmental factors or different emulsion types under same environmental factors.

emulsions had good dispersion without visible difference, which was similar to previous results [45]. When the pH was 7, the emulsion droplets began to aggregate while all dispersed droplets were formed as large aggregates but not destroyed at pH 9. As shown in Fig. 2B, there was no water precipitation and oil phase leakage a pH 2–7 while a large amount of emulsion aggregation and precipitation of aqueous phase at pH 9. This result may relate to the dispersed chitosan in the mobile phase of the emulsion participated in the self-agglomeration of the emulsion droplets leads to a decrease in the emulsion stability of the emulsion [3].

3.2.2. Emulsion physical stability

Emulsion physical stability of CS, CP and CB at different pH values were shown in Fig. 6A. All emulsions had the highest emulsion physical stability at pH 6, which was related to equilibrium between protonation and deprotonation of chitosan, resulting in the formation of sufficient nanoscale aggregated particles to stabilize the emulsion droplets [45]. When the pH of emulsions was <6, the emulsion physical stability decreased together with pH, which were related to the thinning of the interfacial film caused by the dissolution of chitosan particles and the increase of protonation and electrostatic repulsion of amine groups in chitosan [7]. All emulsions had significantly lowest emulsion physical stability at pH 9, which may be related to the coalescence of the droplets which was previously analysed in Section 3.2.1. When coalescence occurred, the macroalgal polyphenols and chitosan in the dispersed phase of the emulsion were bound to the previous droplet surface, resulting in a significant decrease in emulsion physical stability compared to lower pH values. When the pH range was 2–7, the emulsion physical stability of CS was smaller than those of CP and CB, while larger than those of CP and CB at pH 9. The amino groups of chitosan may be deprotonated at pH 9 [46], and the NH_3^+ of chitosan particles and polyphenols were bound by electrostatic interactions (as mentioned in Section 3.1.1), promoting the aggregation of chitosan particles and coalescence of droplets. This enhanced aggregation effect was also observed at pH 10 for Pickering emulsions stabilized by sodium alginate and chitosan [47].

3.2.3. Specific surface area

High specific surface area in emulsions indicate that their droplets have small particle size and high fluidity, contributing to improve the stability of Pickering emulsions [48]. Specific surface area of CS, CP and CB at different pH are shown in Fig. 7A. Specific surface area was at its highest at pH 6 in all emulsions, which would contribute to enhanced emulsion physical stability reported in Section 3.2.2. Previous researches had also appreciated the smaller droplet size and higher specific surface area on the emulsion stability [7,45]. When pH changed, further protonation (pH 2–6) or deprotonation (pH 7–9) of chitosan would lead to changes in the interfacial film formed by chitosan particles located at the oil-water interface, and eventually lead to the reduction of the specific surface area [6,49]. In addition, the specific surface area of the emulsion droplets decreased significantly due to the strong aggregation between droplets at pH 9 (Fig. 2A) which was related to

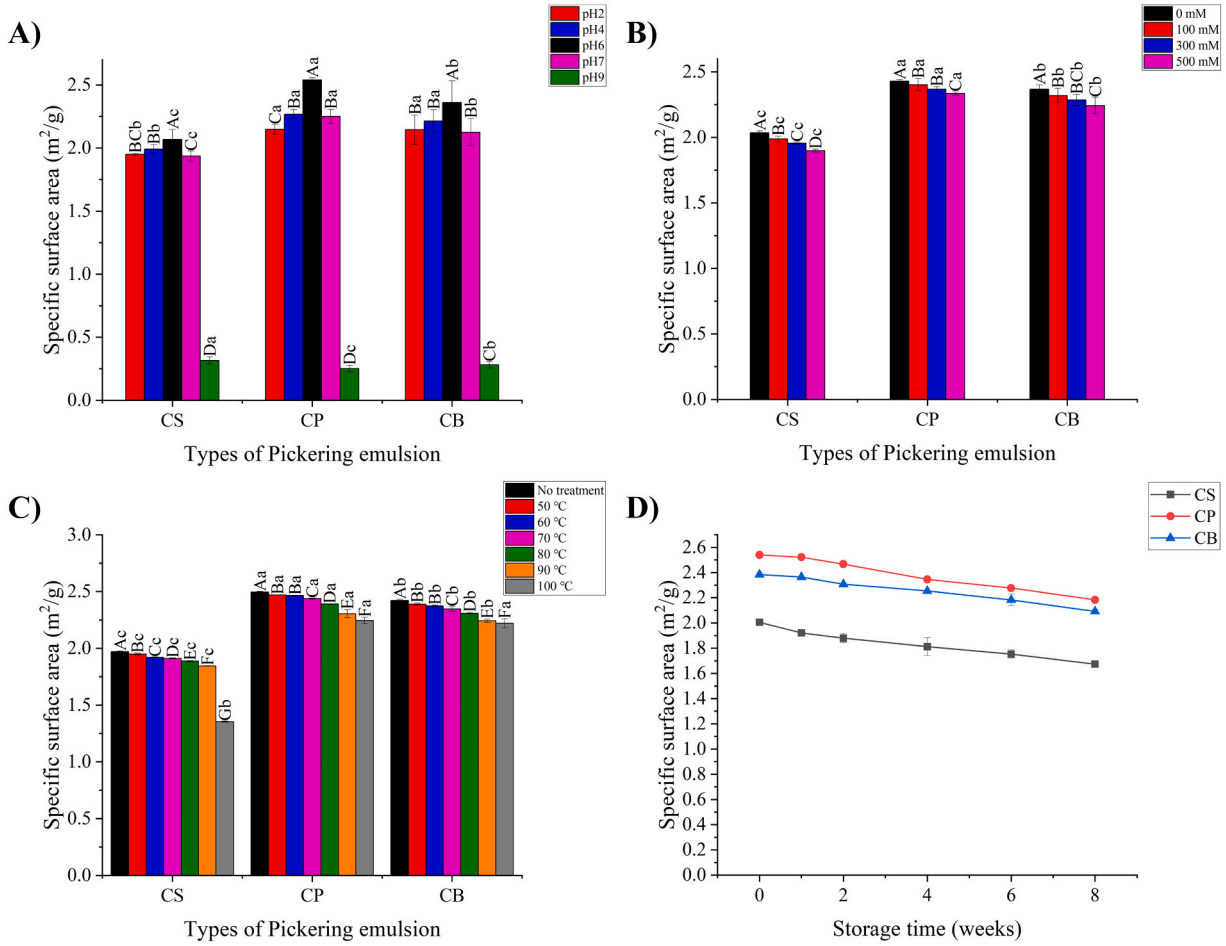

Fig. 7. Specific surface area of Pickering emulsions stabilized with chitosan (CS), chitosan-*Laminaria japonica* polyphenols (CP) and chitosan-*Ascophyllum nodosum* polyphenols (CB) at different (A) pH values (2–9), (B) NaCl concentrations (0–500 mM), (C) heat processing conditions (control, 50–100 °C), (D) storage period (0–8 weeks). Different uppercase or lowercase letters statistically significant differences ($P < 0.05$) in specific surface area within the same emulsion type under different environmental factors or different emulsion types under same environmental factors.

deprotonation of chitosan [3,46].

3.2.4. Rheology

As shown in Fig. 8A, the apparent viscosities of all emulsions at different pH values decreased when increasing the shear rates, suggesting that the emulsions follow a pseudoplastic fluid pattern and exhibit shear-thinning properties. The apparent shear-thinning behaviour of the emulsion was indicative of weak associative interactions, indicating the formation of weak droplet network structures in Pickering emulsions stabilized by chitosan-macroalgal polyphenols [50]. At shear rates of 100 s^{-1}, the apparent viscosity (Fig. 8B) of all emulsion showed the maximum value at pH 9 (23.50 mPa·s (CS), 53.97 mPa·s (CP) and 44.50 mPa·s (CB)), with the second largest value at pH 7 (14.60 mPa·s (CS), 18.13 mPa·s (CP) and 24.50 mPa·s (CB)), minimum at pH 6 (10.37 mPa·s (CS), 11.25 mPa·s (CP) and 11.57 mPa·s (CB)). CP and CB exhibited higher viscosities compared to CS at all pH values, which was attributed to the interaction between chitosan and polyphenols [36]. At pH within the range 2–6, the apparent viscosities of the all emulsions increased with a decrease in pH, which may be due to the chitosan particles originally distributed in the interface layer would be desorbed and dissolved into the dispersed phase due to the protonation of chitosan amino groups [7]. When the pH ranged from 6 to 9, the apparent viscosities of all emulsions showed an increasing trend with the increase of pH. When the pH value is higher than the pKa of chitosan (≈6.8), chitosan aggregated at the droplet interface of the emulsions, leading to the generation of large aggregates of droplets (shown in Fig. 2) and a significant increase in viscosity [51].

3.2.5. TSI

As shown in Fig. 9A, all emulsions had the lowest TSI values at pH 6, which was same with previous results of emulsion physical stability (Section 3.2.2). In the case of pH 9, the TSI value of CS was lower than CP and CB. This could be explained as CP and CB have stronger aggregation effect at this pH, which reduced their stability. For CS, the TSI was greatly affected by pH changes and ordered from highest to lowest the TSI was at its highest at pH 6 followed by pH 7, pH 4, pH 2 and pH 9. These results were consistent with the conclusion of laser particle size analysis experiments (Fig. 7A), the larger the specific surface area could contribute to higher stability of the emulsions. For CP and CB, the TSI values did not varied widely when the pH remained within the range 2–7 and lower than CS, indicating the enhanced stability in low pH. These results may be related to the stable three-dimensional (3D) network of the interface layer [52] that can be created by the combination of chitosan and polyphenols. However, when the pH ranged from 2 to 6, lower pH reflected on higher TSI and poorer stability for all emulsions. With the decrease of pH, the protonation of the amino groups on the d-glucosamine unit, which led to greater electrostatic repulsion and led to the dissolution of the chitosan particles [3,45].

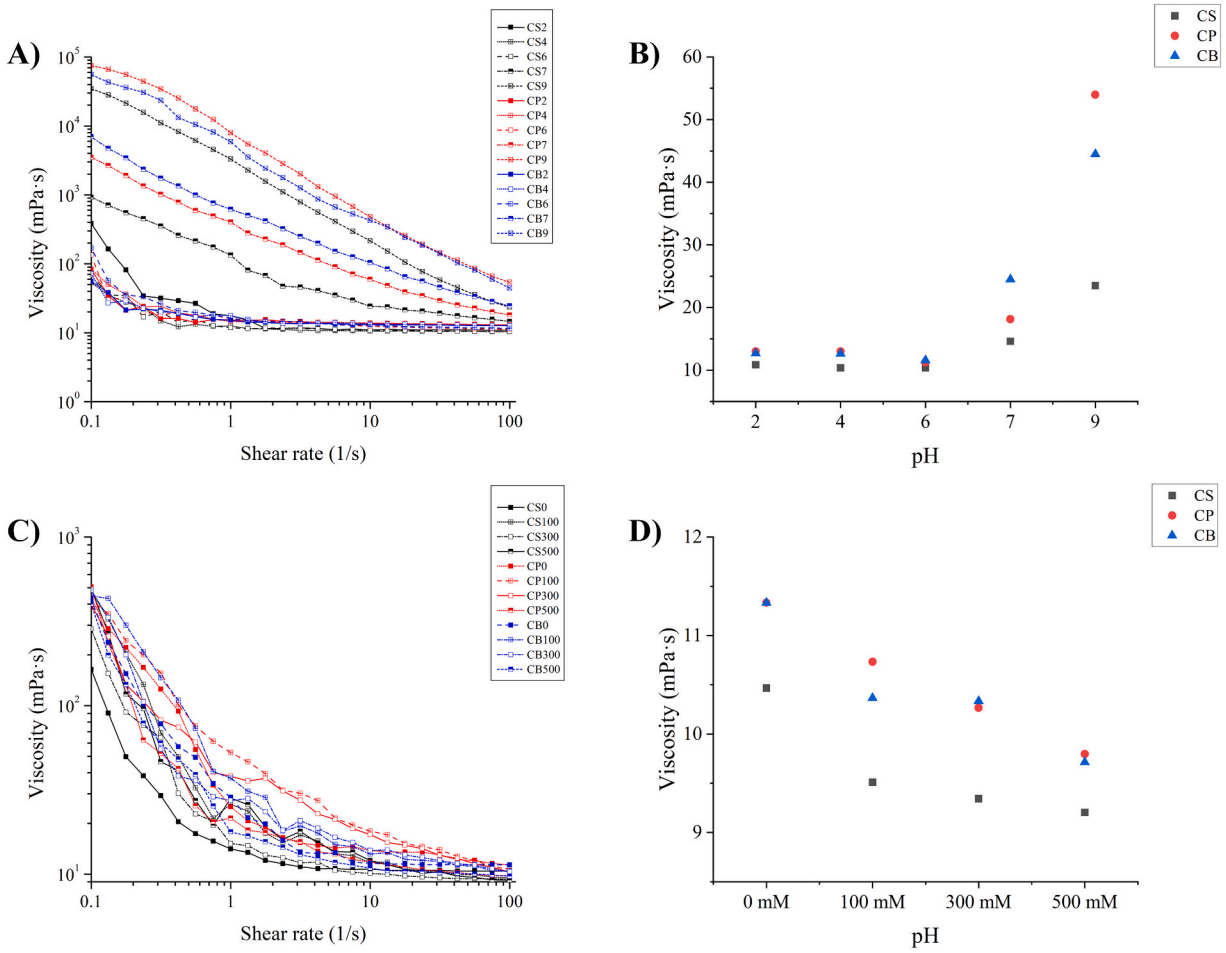

Fig. 8. Rheological properties of Pickering emulsions stabilized with chitosan (CS), chitosan-*Laminaria japonica* polyphenols (CP) and chitosan-*Ascophyllum nodosum* polyphenols (CB) at different pH values (2–9) (A, B) and NaCl concentrations (0–500 mM) (C, D). (A, C) correspond to the flow curves of the emulsions and (B, D) represent their viscosity at a shear rate of 100 s^{-1}.

3.3. Effects of NaCl concentration on emulsion properties

3.3.1. Morphology

The ionic strength could affect the charged particles at the interface between particles of emulsion [38]. This effect was very important in Pickering emulsions prepared by layer-by-layer electrostatic deposition. CP and CB had good dispersion at the NaCl concentration ranged 0–500 mM (Fig. 3A), while CS droplets aggregated at 500 mM NaCl concentration (Fig. 3A). This result indicated that CP and CB had higher stability against ionic strength than CS. Chitosan-based emulsions had lower stability at high NaCl concentrations because NaCl can reduce the charge density of chitosan particles [53]. In the CP and CB, the effect of NaCl concentration on stabilizers may be reduced because of the tighter binding of chitosan and macroalgal polyphenols. It could be found that the three emulsions have no leakage of oil phase or water phase in the NaCl concentration range of 0–500 mM (Fig. 3B) which was same with observation of chitosan-phytic acid-cyclodextrin Pickering emulsion at 0–500 mM NaCl concentration [38].

3.3.2. Emulsion physical stability

Emulsion physical stability of CS, CP and CB at different NaCl concentrations were shown in Fig. 6B. Emulsion physical stability was significantly decreased with the increase of NaCl concentration, which was also observed in some other chitosan-based Pickering emulsions [38,50]. Because of the electrostatic shielding effect at high ionic strength, the electrostatic repulsion between droplets was reduced as NaCl concentration increased, resulting in the enhanced instability of the emulsion [49]. When the NaCl concentration ranged from 0 to 500 mM, CS had lower emulsion physical stability than CP and CB. This was consistent with the conclusion observed in 3.3.1 that the chitosan-macroalgal polyphenols Pickering emulsion had enhanced stability against NaCl concentration stimuli because of tighter network structure.

3.3.3. Specific surface area

The effects of different NaCl concentrations on droplets specific surface area of the emulsions was shown in Fig. 7B. Specific surface area was decreased as NaCl concentration increased, indicating that the droplets of the emulsions were smaller, uniformly distributed, and had the best stability at lower NaCl concentration. This effect of NaCl on the emulsions could also be appreciated in the microscopic observation (Fig. 3A) and emulsion physical stability (Fig. 6B) which was reported in Sections 3.3.1 and 3.3.2, respectively.

3.3.4. Rheology

As shown in Fig. 8C, the apparent viscosity of CS, CP and CB emulsions decreased when increasing the applied shear rates at all NaCl concentrations (0–500 mM), suggesting again the pseudoplastic fluid mode and the shear-thinning properties of these emulsions. At a shear rate of 100 s^{-1} and a NaCl concentration ranging from 0 to 500 mM, the apparent viscosity of each emulsion (Fig. 8D) decreased with the increase of NaCl concentrations, reaching minimum at 500 mM NaCl concentration (9.20 mPa·s (CS), 9.80 mPa·s (CP), and 9.71 mPa·s (CB)), which may be attributed to electrostatic shielding effect at high ionic strength, leading to the aggregation of chitosan and macroalgal

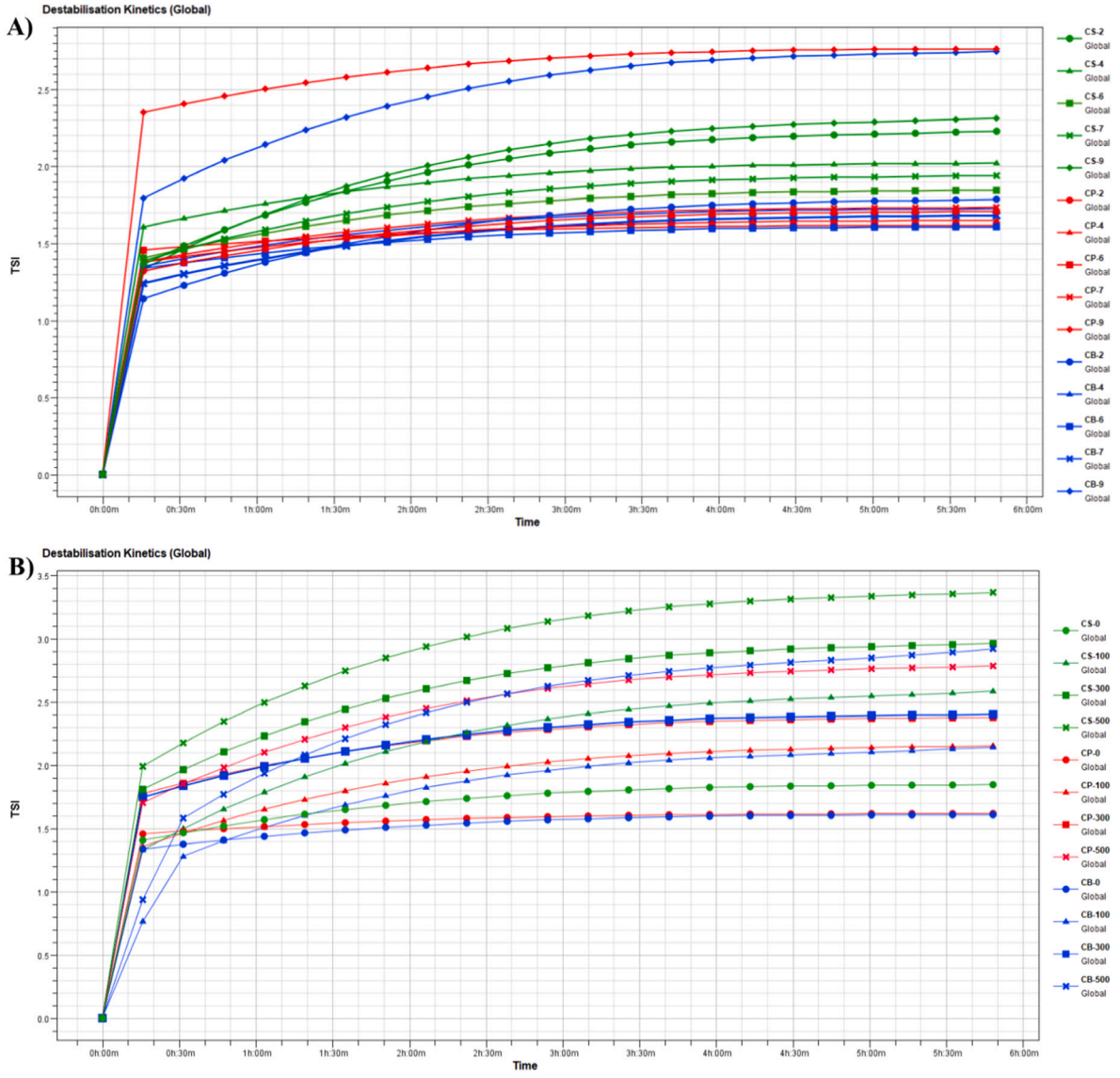

Fig. 9. Turbiscan stability index (TSI) of Pickering emulsions stabilized with chitosan (CS), chitosan-*Laminaria japonica* polyphenols (CP) and chitosan-*Ascophyllum nodosum* polyphenols (CB) at different (A) pH values (2–9) and (B) NaCl concentrations (0–500 mM).

polyphenols on the surface of the emulsion droplets [54]. This results in a reduction of the distribution of chitosan and macroalgal polyphenols in the continuous phase, which further reduces the viscosity of the emulsion. At all NaCl concentrations, CP and CB exhibited higher viscosity compared to CS, indicating stronger molecular interactions between chitosan and polyphenols and promoted cross-linking [49].

3.3.5. TSI

TSI value of CS was higher than that of CP and CB at all NaCl concentrations studied, indicating lower stability of the emulsions at higher ionic strength conditions (Fig. 9B). This phenomenon indicated that the addition of macroalgal polyphenols would contribute to the improvement of emulsion stability, which may because of enhanced 3D network. For CS, CP, and CB, the TSI stability was greatly affected by the change of NaCl concentration. With the increase of NaCl concentration, the TSI stability of the three emulsions decreased which was same with the trend of emulsion physical stability reported in Section 3.3.2.

3.4. Effects of heat treatment on emulsion properties

3.4.1. Morphology

Since many foods processing and preservation require high temperature treatment, it was very important for the formulated emulsion samples to have high temperature stability in practical applications [47]. As shown in Fig. 4, when the three emulsions were not heat-treated, the droplets (green) of the emulsions had good distribution, and there was no tendency for the emulsion droplets to aggregate. When the heat treatment temperature was 50 °C, CS began to show the tendency of droplet aggregation. Droplets of CP and CB began to aggregate at higher temperature (80 °C). When CS was heat-treated at 100 °C for 30 min, the emulsion droplets broke up and formed larger droplets, while the droplets of CP and CB did not form a similar droplet state. The charge on the chitosan surface increased and became more hydrophilic at increased temperature, at the same time, the kinetic energy of the chitosan particles increased, and the Brownian motion leaded to the desorption and redistribution of the particles, which promoted droplets collision and coalescence [3]. CP and CB had significantly better droplet distribution than CS at all treatments, indicating that the addition of macroalgal polyphenols could reduce droplets aggregation against high

temperature treatment.

3.4.2. Physical stability

Emulsion physical stability of CS, CP and CB at different heat processing conditions are shown in Fig. 6C. Emulsions without heat treatment had the highest emulsion physical stability. As the temperature of heat treatment increased, all types of emulsions had significantly lower emulsion physical stability, indicating that heat treatment could significantly weaken the stability of all emulsions, as aggregation of droplets reported in Section 3.4.1. The decrease trend of emulsion stability as increased temperature was similar to that of [10] for Pickering emulsion stabilized by chitosan-gum Arabic nanoparticle. After heat treatments of 100 °C water bath for 30 min, the emulsion physical stability of CS (10.67 %) was significantly lower than CP and CB (95.00 %). The increase in physical stability of CP and CB may be related to the droplet aggregation resistance provided by the addition of macroalgal polyphenols reported in Section 3.4.1.

3.4.3. Specific surface area

The effects of different heat treatments on the specific surface area of emulsions were represented in Fig. 7C. The variations of the specific surface area of the emulsion droplets were similar to the emulsion physical stability (Fig. 6C). During the temperature increase, the generation of large-sized droplets (Fig. 4) resulted in a significant decrease in the specific surface area of the emulsion. It is worth noting that the specific surface area of CP (2.25 m^2/g) and CB (2.22 m^2/g) were much higher than that of CS (1.35 m^2/g) even after heat treatments at 100 °C. This phenomenon suggested that CP and CB maintained the specific surface area and fluidity of emulsions than that of CS more attractively.

3.5. Effects of storage on emulsion properties

3.5.1. Morphology

Storage stability determined to a certain extent whether the food product can be widely used [50]. The microstate and macroscopic observations of the emulsions stored at pH 6 during 8 weeks are shown in Fig. 5A and B, respectively. Overall, the droplets had a good distribution in all the emulsions after 1 week of storage, with increased tendency to aggregation with increased storage time. CS droplets aggregated after 2 weeks of storage, while both CP and CB started to aggregate after 4 weeks of storage, showing higher stability compared to CS. At the end of 8-week storage, CS showed significant droplet aggregation compared to that of CP and CB (Fig. 5A). Meanwhile, a small amount of water phase separation at the bottom of the CS at 6 weeks storage while no water phase separation at 8 weeks storage for CP and CB (Fig. 5B). All these observations indicate that the addition of macroalgal polyphenols could contribute to improve the droplet distribution of chitosan-based Pickering emulsions over an 8-week storage period.

3.5.2. Emulsion physical stability

Emulsion physical stability of CS, CP and CB at different storage periods are shown in Fig. 6D. Emulsion physical stability of all emulsions showed a decreasing trend with the prolongation of storage time. This is also consistent with the conclusion obtained from the macroscopic aqueous phase separation and microscopic droplets aggregation observed in Section 3.5.1. The emulsion physical stability of CS showed a significant downward trend after 4 weeks of storage, resulting in the destruction of the original steric hindrance because of droplets aggregation. This result was consistent with the conclusions previously reported for chitosan-stabilized Pickering emulsions by [45], which related to the rupture of the chitosan particle layer leading to emulsion flocculation. After 8 weeks of storage, the emulsion physical stability of CS was only 38.33 %, which was significantly lower than that of CP (88.67 %) and CB (87.67 %), respectively. During the 8-week storage period, CS showed consistently lower emulsion physical stability compared to CP and CB, indicating that CS had worse stability against aggregation.

3.5.3. Specific surface area

The effect of different storage periods on the specific surface area of emulsions could be observed in Fig. 7D. Overall, the specific surface area of all emulsions decreased at increased storage time. After 8 weeks of storage, CS decreased from 2.01 m^2/g to 1.67 m^2/g, CP decreased from 2.54 m^2/g to 2.18 m^2/g, and CB decreased from 2.38 m^2/g to 2.09 m^2/g. The increase in specific surface area may be due to the aggregation of small droplets to form aggregates with larger particle size (shown in Fig. 5A), which was also found by [45] in chitosan particle stabilized Pickering emulsion. The combination of chitosan and macroalgal polyphenols could support a more stable interface layer and provide a larger specific surface area and better long-term storage.

4. Conclusions

In this research, polyphenols from different variety of macroalgal were used to generate chitosan-macroalgal polyphenol Pickering emulsion. FTIR, XRD, contact angle, and TEM results indicated that macroalgal polyphenols could bind to the amorphous regions of chitosan particles through hydrogen bonding and electrostatic interactions to jointly stabilize the emulsion. Emulsions stabilized by macroalgal polyphenols and chitosan had increased stability at pH ranged 2–7, NaCl concentrations ranged from 0 to 500 mM), heat treatments within the 50–100 °C range, and can be stored up to 8-weeks. Moreover, the pseudoplastic behaviour of chitosan and chitosan-polyphenols Pickering emulsions were observed at different pH and NaCl concentrations. This research provided complete and effective support for the utilization and application of Pickering emulsions stabilized with chitosan and chitosan-macroalgal polyphenols. It exhibited complete analysis of the behaviour of these emulsions of the stability to external environmental stimuli. Current results are necessary for the practical application of these emulsions to enhance the protection of different bioactive molecules that could be useful in the pharmaceutical, nutraceutical, and functional food industries. In the following studies, more research interests should focus on the protective effect of this chitosan-macroalgal polyphenol Pickering emulsion on various bioactive components, and explore the application in industrial production.

Statement of informed consent, human/animal rights

No conflicts, informed consent, or human or animal rights were applicable to this study.

CRediT authorship contribution statement

Weihao Meng: References collection, Software, Validation, Visualization and Writing–original draft and editing.

Hongnan Sun: Methodology, Supervision, and Writing-review and editing.

Taihua Mu: Conceptualization, Supervision, and Writing-review.

Marco Garcia Vaquero: Supervision, and Writing-review.

Declaration of competing interest

The authors declare that they have no known competing financial interests or personal relationships that could have appeared to influence the work reported in this paper.

Acknowledgements

Weihao Meng is currently in receipt of a PhD Scholarship within the joint collaborative PhD programme between UCD and GSCAAS. This study is funded by the Science and Technology Innovation Project of Chinese Academy of Agricultural Sciences (CAAS-ASTIP-202X-IFST).

References

[1] T. Xia, C. Xue, Z. Wei, Physicochemical characteristics, applications and research trends of edible Pickering emulsions, Trends Food Sci. Technol. 107 (2021) 1–15, https://doi.org/10.1016/j.tifs.2020.11.019.
[2] M. Shahbazi, H. Jäger, R. Ettelaie, Development of an antioxidative Pickering emulsion gel through polyphenol-inspired free-radical grafting of microcrystalline cellulose for 3D food printing, Biomacromolecules 22 (2021) 4592–4605, https://doi.org/10.1021/acs.biomac.1c00896.
[3] W.W. Mwangi, K.W. Ho, B.T. Tey, E.S. Chan, Effects of environmental factors on the physical stability of Pickering-emulsions stabilized by chitosan particles, Food Hydrocoll. 60 (2016) 543–550, https://doi.org/10.1016/j.foodhyd.2016.04.023.
[4] B.R. Shah, P. Dvořák, J. Velíšek, J. Mráz, Opening a new gateway towards the applications of chitosan nanoparticles stabilized Pickering emulsion in the realm of aquaculture, Carbohydr. Polym. 265 (2021), 118096, https://doi.org/10.1016/j.carbpol.2021.118096.
[5] H. Boroumand, F. Badie, S. Mazaheri, Z.S. Seyedi, J.S. Nahand, M. Nejati, H. B. Baghi, M. Abbasi-Kolli, B. Badehnoosh, M. Ghandali, M.R. Hamblin, H. Mirzaei, Chitosan-based nanoparticles against viral infections, Front. Cell. Infect. Microbiol. 11 (2021) 1–22, https://doi.org/10.3389/fcimb.2021.643953.
[6] Q. Zhao, L. Fan, Y. Liu, J. Li, Recent advances on formation mechanism and functionality of chitosan-based conjugates and their application in o/w emulsion systems: a review, Food Chem. 380 (2022), 131838, https://doi.org/10.1016/j.foodchem.2021.131838.
[7] M. Atarian, A. Rajaei, M. Tabatabaei, A. Mohsenifar, H. Bodaghi, Formulation of Pickering sunflower oil-in-water emulsion stabilized by chitosan-stearic acid nanogel and studying its oxidative stability, Carbohydr. Polym. 210 (2019) 47–55, https://doi.org/10.1016/j.carbpol.2019.01.008.
[8] A. Sharkawy, M.F. Barreiro, A.E. Rodrigues, Chitosan-based Pickering emulsions and their applications: a review, Carbohydr. Polym. 250 (2020), 116885, https://doi.org/10.1016/j.carbpol.2020.116885.
[9] T. Aoki, E.A. Decker, D.J. McClements, Influence of environmental stresses on stability of O/W emulsions containing droplets stabilized by multilayered membranes produced by a layer-by-layer electrostatic deposition technique, Food Hydrocoll. 19 (2005) 209–220, https://doi.org/10.1016/j.foodhyd.2004.05.006.
[10] J. Han, F. Chen, C. Gao, Y. Zhang, X. Tang, Environmental stability and curcumin release properties of Pickering emulsion stabilized by chitosan/gum arabic nanoparticles, Int. J. Biol. Macromol. 157 (2020) 202–211, https://doi.org/10.1016/j.ijbiomac.2020.04.177.
[11] P. Lv, D. Wang, Y. Chen, S. Zhu, J. Zhang, L. Mao, Y. Gao, F. Yuan, Pickering emulsion gels stabilized by novel complex particles of high-pressure-induced WPI gel and chitosan: fabrication, characterization and encapsulation, Food Hydrocoll. 108 (2020), 105992, https://doi.org/10.1016/j.foodhyd.2020.105992.
[12] M. Jo, C. Ban, K.K.T. Goh, Y.J. Choi, Enhancement of the gut-retention time of resveratrol using waxy maize starch nanocrystal-stabilized and chitosan-coated Pickering emulsions, Food Hydrocoll. 112 (2021), 106291, https://doi.org/10.1016/j.foodhyd.2020.106291.
[13] M.H. Asfour, H. Elmotasem, D.M. Mostafa, A.A.A. Salama, Chitosan based Pickering emulsion as a promising approach for topical application of rutin in a solubilized form intended for wound healing: in vitro and in vivo study, Int. J. Pharm. 534 (2017) 325–338, https://doi.org/10.1016/j.ijpharm.2017.10.044.
[14] Y. Ji, C. Han, E. Liu, X. Li, X. Meng, B. Liu, Pickering emulsions stabilized by pea protein isolate-chitosan nanoparticles: fabrication, characterization and delivery EPA for digestion in vitro and in vivo, Food Chem. 378 (2022), 132090, https://doi.org/10.1016/j.foodchem.2022.132090.
[15] R.S. Hosseini, A. Rajaei, Potential Pickering emulsion stabilized with chitosan-stearic acid nanogels incorporating clove essential oil to produce fish-oil-enriched mayonnaise, Carbohydr. Polym. 241 (2020), 116340, https://doi.org/10.1016/j.carbpol.2020.116340.
[16] B.R. Shah, Y. Li, W. Jin, Y. An, L. He, Z. Li, W. Xu, B. Li, Preparation and optimization of Pickering emulsion stabilized by chitosan-tripolyphosphate nanoparticles for curcumin encapsulation, Food Hydrocoll. 52 (2016) 369–377, https://doi.org/10.1016/j.foodhyd.2015.07.015.
[17] W. Meng, T. Mu, H. Sun, M. Garcia-Vaquero, Evaluation of the chemical composition and nutritional potential of brown macroalgae commercialised in China, Algal Res. 64 (2022), 102683, https://doi.org/10.1016/j.algal.2022.102683.
[18] L. Ford, A.C. Stratakos, K. Theodoridou, J.T.A. Dick, G.N. Sheldrake, M. Linton, N. Corcionivoschi, P.J. Walsh, Polyphenols from Brown seaweeds as a potential antimicrobial agent in animal feeds, ACS Omega 5 (2020) 9093–9103, https://doi.org/10.1021/acsomega.9b03687.
[19] C. Jimenez-Lopez, A.G. Pereira, C. Lourenço-Lopes, P. Garcia-Oliveira, L. Cassani, M. Fraga-Corral, M.A. Prieto, J. Simal-Gandara, Main bioactive phenolic compounds in marine algae and their mechanisms of action supporting potential health benefits, Food Chem. 341 (2021), 128262, https://doi.org/10.1016/j.foodchem.2020.128262.
[20] H.J. Kim, H.I. Yong, B.W. Lee, S. Park, K.H. Baek, T.H. Kim, C. Jo, Plasma-polymerized phlorotannins and their enhanced biological activities, J. Agric. Food Chem. 68 (2020) 2357–2365, https://doi.org/10.1021/acs.jafc.9b07077.
[21] S.R. Park, J.H. Kim, H.D. Jang, S.Y. Yang, Y.H. Kim, Inhibitory activity of minor phlorotannins from ecklonia cava on α-glucosidase, Food Chem. 257 (2018) 128–134, https://doi.org/10.1016/j.foodchem.2018.03.013.
[22] M. Dutot, E. Olivier, S. Fouyet, R. Magny, K. Hammad, E. Roulland, P. Rat, R. Fagon, In vitro chemopreventive potential of phlorotannins-rich extract from Brown algae by inhibition of Benzo[a]pyrene-induced P2X7 activation and toxic effects, Mar. Drugs 19 (2021) 1–12, https://doi.org/10.3390/md19010034.
[23] W. Meng, T. Mu, H. Sun, M. Garcia-Vaquero, Phlorotannins: a review of extraction methods, structural characteristics, bioactivities, bioavailability, and future trends, Algal Res. 60 (2021), 102484, https://doi.org/10.1016/j.algal.2021.102484.
[24] W. Meng, H. Sun, T. Mu, M. Garcia-Vaquero, Pickering emulsions with chitosan and macroalgal polyphenols stabilized by layer-by-layer electrostatic deposition, Carbohydr. Polym. 300 (2022), 120256, https://doi.org/10.1016/j.carbpol.2022.120256.
[25] S. Wang, D. Qu, G. Zhao, L. Yang, L. Zhu, H. Song, H. Liu, Characterization of the structure and properties of the isolating interfacial layer of oil–water emulsions stabilized by soy hull polysaccharide: effect of pH changes, Food Chem. 370 (2022), 131029, https://doi.org/10.1016/j.foodchem.2021.131029.
[26] L. Yang, X. Cao, A. Gai, X. Qiao, Z. Wei, J. Li, J. Xu, C. Xue, Chitosan/guar gum nanoparticles to stabilize Pickering emulsion for astaxanthin encapsulation, LWT 165 (2022), 113727, https://doi.org/10.1016/j.lwt.2022.113727.
[27] J. Chen, T. Mu, M. Zhang, D. Goffin, Effect of high hydrostatic pressure on the structure, physicochemical and functional properties of protein isolates from cumin (Cuminum cyminum) seeds, Int. J. Food Sci. Technol. 54 (2019) 752–761, https://doi.org/10.1111/ijfs.13990.
[28] X. Zhu, J. Chen, Y. Hu, N. Zhang, Y. Fu, X. Chen, Tuning complexation of carboxymethyl cellulose/cationic chitosan to stabilize Pickering emulsion for curcumin encapsulation, Food Hydrocoll. 110 (2021), 106135, https://doi.org/10.1016/j.foodhyd.2020.106135.
[29] N. Kasiri, M. Fathi, Production of cellulose nanocrystals from pistachio shells and their application for stabilizing Pickering emulsions, Int. J. Biol. Macromol. 106 (2018) 1023–1031, https://doi.org/10.1016/j.ijbiomac.2017.08.112.
[30] N.M. Khan, T.H. Mu, M. Zhang, L.A. Arogundade, The effects of pH and high hydrostatic pressure on the physicochemical properties of a sweet potato protein emulsion, Food Hydrocoll. 35 (2014) 209–216, https://doi.org/10.1016/j.foodhyd.2013.05.011.
[31] X. Tong, J. Cao, M. Sun, P. Liao, S. Dai, W. Cui, X. Cheng, Y. Li, L. Jiang, H. Wang, Physical and oxidative stability of oil-in-water (O/W) emulsions in the presence of protein (peptide): characteristics analysis and bioinformatics prediction, LWT 149 (2021), 111782, https://doi.org/10.1016/j.lwt.2021.111782.
[32] X. Cai, Y. Wang, X. Du, X. Xing, G. Zhu, Stability of pH-responsive Pickering emulsion stabilized by carboxymethyl starch/xanthan gum combinations, Food Hydrocoll. 109 (2020), 106093, https://doi.org/10.1016/j.foodhyd.2020.106093.
[33] Y.V. García-Tejeda, E.J. Leal-Castañeda, V. Espinosa-Solis, V. Barrera-Figueroa, Synthesis and characterization of rice starch laurate as food-grade emulsifier for canola oil-in-water emulsions, Carbohydr. Polym. 194 (2018) 177–183, https://doi.org/10.1016/j.carbpol.2018.04.029.
[34] B. Niu, H. Chen, W. Wu, X. Fang, H. Mu, Y. Han, H. Gao, Co-encapsulation of chlorogenic acid and cinnamaldehyde essential oil in Pickering emulsion stablized by chitosan nanoparticles, Food Chem. X 14 (2022), 100312, https://doi.org/10.1016/j.fochx.2022.100312.
[35] S. Kumari, P. Rath, A.Sri Hari Kumar, T.N. Tiwari, Extraction and characterization of chitin and chitosan from fishery waste by chemical method, Environ. Technol. Innov. 3 (2015) 77–85, https://doi.org/10.1016/j.eti.2015.01.002.
[36] X. Zhu, X. Hou, B. Ma, H. Xu, Y. Yang, Chitosan/gallnut tannins composite fiber with improved tensile, antibacterial and fluorescence properties, Carbohydr. Polym. 226 (2019), 115311, https://doi.org/10.1016/j.carbpol.2019.115311.
[37] H. Staroszczyk, K. Sztuka, J. Wolska, I. Kołodziejska, A. Wojtasz-Pająk, Interactions of fish gelatin and chitosan in uncrosslinked and crosslinked with EDC films: FT-IR study, Spectrochim. Acta A Mol. Biomol. Spectrosc. 117 (2014) 707–712, https://doi.org/10.1016/j.saa.2013.09.044.
[38] J. Lu, X. Li, C. Qiu, D.J. McClements, A. Jiao, J. Wang, Z. Jin, Preparation and characterization of food-grade Pickering emulsions stabilized with chitosan-phytic acid-cyclodextrin nanoparticles, Foods 11 (2022) 450, https://doi.org/10.3390/foods11030450.
[39] K. Okano, T. Minagawa, J. Yang, M. Shimojoh, K. Kurita, Amorphous reprecipitated chitosan as a novel morphological form, Polym. Bull. 62 (2009) 119–126, https://doi.org/10.1007/s00289-008-0002-2.
[40] R. Yoksan, J. Jirawutthiwongchai, K. Arpo, Encapsulation of ascorbyl palmitate in chitosan nanoparticles by oil-in-water emulsion and ionic gelation processes, Colloids Surf. B: Biointerfaces 76 (2010) 292–297, https://doi.org/10.1016/j.colsurfb.2009.11.007.
[41] M. Sultan, H. Elsayed, A.E.F. Abdelhakim, G. Taha, Active packaging gelatin films based on chitosan/Arabic gum/coconut oil Pickering nano emulsions, J. Appl. Polym. Sci. 139 (2022) 1–18, https://doi.org/10.1002/app.51442.
[42] P. Senthilkumar, G. Yaswant, S. Kavitha, E. Chandramohan, G. Kowsalya, R. Vijay, B. Sudhagar, D.S.R.S. Kumar, Preparation and characterization of hybrid chitosan-silver nanoparticles (Chi-ag NPs); a potential antibacterial agent, Int. J. Biol. Macromol. 141 (2019) 290–297, https://doi.org/10.1016/j.ijbiomac.2019.08.234.
[43] M. Tabatabaei, B. Ebrahimi, A. Rajaei, Producing submicron chitosan-stabilized oil Pickering emulsion powder by an electrostatic collector-equipped spray dryer, Carbohydr. Polym. 294 (2022), 119791, https://doi.org/10.1016/j.carbpol.2022.119791.
[44] Y. Yang, Z. Fang, X. Chen, W. Zhang, Y. Xie, Y. Chen, Z. Liu, W. Yuan, An overview of Pickering emulsions: solid-particle materials, classification, morphology, and applications, Front. Pharmacol. 8 (2017) 1–20, https://doi.org/10.3389/fphar.2017.00287.
[45] R.A. Bhutto, M. Wang, Z. Qi, N.U.A. Hira, J. Jiang, H. Zhang, S. Iqbal, J. Wang, M. A.C. Stuart, X. Guo, Pickering emulsions based on the pH-responsive assembly of food-grade chitosan, ACS Omega 6 (2021) 17915–17922, https://doi.org/10.1021/acsomega.1c01490.
[46] H. İlyasoğlu, M. Nadzieja, Z. Guo, Caffeic acid grafted chitosan as a novel dual-functional stabilizer for food-grade emulsions and additive antioxidant property,

Food Hydrocoll. 95 (2019) 168–176, https://doi.org/10.1016/j.foodhyd.2019.04.043.

[47] Y. Tang, C. Gao, Y. Zhang, X. Tang, The microstructure and physiochemical stability of Pickering emulsions stabilized by chitosan particles coating with sodium alginate: influence of the ratio between chitosan and sodium alginate, Int. J. Biol. Macromol. 183 (2021) 1402–1409, https://doi.org/10.1016/j.ijbiomac.2021.05.098.

[48] Y. Ming, Y. Xia, G. Ma, Aggregating particles on the O/W interface: tuning pickering emulsion for the enhanced drug delivery systems, Aggregate (2022) 1–19, https://doi.org/10.1002/agt2.162.

[49] F. Zhang, X. Cai, L. Ding, S. Wang, Effect of pH, ionic strength, chitosan deacetylation on the stability and rheological properties of O/W emulsions formulated with chitosan/casein complexes, Food Hydrocoll. 111 (2021), 106211, https://doi.org/10.1016/j.foodhyd.2020.106211.

[50] X.M. Li, Q.T. Xie, J. Zhu, Y. Pan, R. Meng, B. Zhang, H.Q. Chen, Z.Y. Jin, Chitosan hydrochloride/carboxymethyl starch complex nanogels as novel Pickering stabilizers: physical stability and rheological properties, Food Hydrocoll. 93 (2019) 215–225, https://doi.org/10.1016/j.foodhyd.2019.02.021.

[51] J. Blockx, A. Verfaillie, W. Thielemans, K. Muylaert, Unravelling the mechanism of chitosan-driven flocculation of microalgae in seawater as a function of pH, ACS Sustain. Chem. Eng. 6 (2018) 11273–11279, https://doi.org/10.1021/acssuschemeng.7b04802.

[52] R. Zhang, L. Li, C. Ma, F. Ezzahra Ettoumi, M. Javed, X. Lin, X. Shao, G. Xiao, Z. Luo, Shape-controlled fabrication of zein and peach gum polysaccharide based complex nanoparticles by anti-solvent precipitation for curcumin-loaded Pickering emulsion stabilization, Sustain. Chem. Pharm. 25 (2022), 100565, https://doi.org/10.1016/j.scp.2021.100565.

[53] U. Klinkesorn, The role of chitosan in emulsion formation and stabilization, Food Rev. Int. 29 (2013) 371–393, https://doi.org/10.1080/87559129.2013.818013.

[54] M. Lundin, L. Macakova, A. Dedinaite, P. Claesson, Interactions between chitosan and SDS at a low-charged silica substrate compared to interactions in the bulk - the effect of ionic strength, Langmuir 24 (2008) 3814–3827, https://doi.org/10.1021/la702653m.